Neurochemical Research (2022) 47:3261–3271
https://doi.org/10.1007/s11064-022-03675-0

ORIGINAL PAPER

Panax notoginseng Saponins Protect Brain Microvascular Endothelial Cells against Oxygen-Glucose Deprivation/Resupply-Induced Necroptosis via Suppression of RIP1-RIP3-MLKL Signaling Pathway

Yanhong Hu[1,2] · Hongtao Lei[2] · Sai Zhang[1] · Jiabao Ma[1] · Soyeon Kang[1] · Liangqin Wan[1] · Fanghe Li[1] · Fan Zhang[1] · Tianshi Sun[1] · Chujun Zhang[1] · Weihong Li[3]

Received: 23 February 2022 / Revised: 29 June 2022 / Accepted: 1 July 2022 / Published online: 29 July 2022

Abstract

Recently, necroptosis has emerged as one of the important mechanisms of ischemia stroke. Necroptosis can be rapidly activated in endothelial cells to cause vascular damage and neuroinflammation. *Panax notoginseng* saponins (PNS), an ingredient extracted from the root of *Panax notoginseng* (Burk.) F.H. Chen, was commonly used for ischemic stroke, while its molecular mechanism and targets have not been fully clarified. Our study aimed to clarify the anti-necroptosis effect of PNS by regulating RIP1-RIP3-MLKL signaling pathway in brain microvascular endothelial cells (BMECs) subjected to transient oxygen-glucose deprivation (OGD/resupply [R]). In vitro, the necroptosis model of rat BMECs was established by testing the effect of OGD/R in the presence of the pan-caspase inhibitor z-VAD-FMK. After administration of PNS and Nec-1, cell viability, cell death modality, the expression of RIP1-RIP3-MLKL pathway and mitochondrial membrane potential (Δψm) level were investigated in BMECs upon OGD/R injury. The results showed that PNS significantly enhanced cell viability of BMECs determined by CCK-8 analysis, and protected BMECs from necroptosis by Flow cytometry and TEM. In addition, PNS inhibited the phosphorylation of RIP1, RIP3, MLKL and the downstream expression of PGAM5 and Drp1, while similar results were observed in Nec-1 intervention. We further investigated whether PNS prevented the Δψm depolarization. Our current findings showed that PNS effectively reduced the occurrence of necroptosis in BMECs exposed to OGD/R by inhibition of the RIP1-RIP3-MLK signaling pathway and mitigation of mitochondrial damage. This study provided a novel insight of PNS application in clinics.

Keywords Necroptosis · RIP1-RIP3-MLKL signaling pathway · *Panax notoginseng* saponin (PNS) · Oxygen-glucose deprivation/resupply (OGD/R) · Brain microvascular endothelial cells (BMECs)

Introduction

Stroke includes hemorrhagic stroke and ischemic stroke, the latter accounts for ~87% in total stroke events [1]. Studies have shown that reperfusion in ischemic areas can cause severe brain injury and related dysfunction, which also called cerebral ischemia-reperfusion injury (CIRI). CIRI is a complex pathophysiological process by a series of mechanism. Brain microvascular endothelial cells (BMECs) play an important role in the microenvironment of CIRI. Dysfunction and death of BMECs not only promote neuroinflammation and brain edema, but also increase the risk of intracerebral hemorrhage of thrombolytic therapies [2]. Multiple cell death mechanisms, including necrosis, apoptosis, and autophagy, occur in the pathogenesis of CIRI. Previously, necrosis was considered a type of non-programed cell death differing from apoptosis, which was regulated by caspase cascades. Recent studies have demonstrated that necrotic cell death may be a regulated process known as

✉ Weihong Li
liweihong.403@163.com

1 School of Traditional Chinese Medicine, Beijing University of Chinese Medicine, 100029 Beijing, China

2 Experimental Research Center, China Academy of Chinese Medical Sciences, 100700 Beijing, China

3 School of Nursing, Beijing University of Chinese Medicine, No 11 Bei San Huan Dong Road, Chao Yang District, 100029 Beijing, China

necroptosis [3]. On brain ischemic conditions, necroptosis can be rapidly activated in endothelial cells to cause vascular damage and neuroinflammation [4]. Therefore, necroptosis can provide a new insight into the pathogenesis of CIRI and suggest a new potential therapeutic target for vascular protection and neuroprotection. Though the mechanism of necroptosis are not fully understood, it is generally accepted that the occurrence of necroptosis depends on the activation of receptor interaction protein kinase-1(RIP1)-receptor interaction protein kinase-3(RIP3)-mixed lineage kinase domain-like protein (MLKL) pathway [5].

Although diagnosis and treatment of CIRI has made great progress in the past decades, treatment methods remain limited [6]. Traditional Chinese medicine (TCM) can intervene multiple targets and pathways in CIRI pathological process, with few side effects. *Panax notoginseng* (Burk.) F.H. Chen (known as Sanqi), one of the most popular Chinese herbs, has been widely used to treat ischemic stroke and cardiovascular disorders in TCM. *Panax notoginseng* saponins (PNS), an active ingredient extracted from the root of *Panax notoginseng* (Burk.) F.H. Chen, has many pharmacological effects, including cerebral vasodilation, anti-inflammation, neuron protection, attenuation of apoptosis and caspase activation, reduction of cytokines and blood-brain barrier permeability improvement against CIRI in vivo and in vitro [7, 8]. In addition, Xuesaitong, a neuroprotective injection in which PNS is the main pharmacodynamic component, has been widely used in the treatment of stroke in China for many years [9]. Moreover, the efficacy and safety of PNS in patients with non-minor acute ischemic stroke had been assess by a random controlled trial [10]. But the molecular targets and pathways regulated by PNS remains unclear. In the early stage, animal and cell experiments were used to study the pharmacodynamic characteristics and the mechanism of PNS on cerebral ischemic injury [11, 12]. However, little is known about how PNS improves the recovery of cerebral microvascular function via regulation of the RIP1-RIP3-MLKL necroptosis signaling pathway. Hence, this study aims to explore whether PNS reduces the brain injury of stroke by targeting the RIP1-RIP3-MLKL pathway and subsequently preventing BMECs necroptosis.

Materials and Methods

Materials

Aur and pan caspase inhibitor z-Val-Ala-Dl-Asp (OMe)-fluoromethylketone (z-VAD-FMK) and Necrostatin-1 (Nec-1) were purchased from Enzo Life Sciences International, Inc. (Farmingdale, New York, USA). Cell Counting Kit 8 (CCK-8) was purchased from DOJINDO Laboratories (Dojindo, Japan). Annexin V-fluorescein isothiocyanate (FITC)/propidium iodide (PI) double staining kit was purchased from BD Biosciences Pharmingen (BD Biosciences, NJ, USA). RIP1, p-RIP1(Ser166), p-MLKL(Ser358) and dynamin-related protein 1 (Drp1) antibodies were purchased from Cell Signaling Technology (Danvers, MA, USA). RIP3, p-RIP3(T231 + S232), MLKL and phosphoglycerate mutase family member 5 (PGAM5) antibody were purchased from Abcam (Cambridge, UK). Secondary antibodies were purchased from Beijing Zhongshan Golden Bridge Biotechnology (Beijing, China). PNS was purchased from Chengdu Manst Biotechnology (Chengdu, China), composed of Notoginsenoside R1 7.4%, ginsenoside Rg1 26.3%, ginsenoside Re 3.7%, ginsenoside Rb1 27.7%, ginsenoside Rd 7.6%.

Preparation of Rat BMECs and Necroptosis Model

Primary rat BMECs were obtained from male Sprague-Dawley (SD) rats (grade SPF/VAF), weighing about 20 g (Beijing Vital River Laboratory Animals Co., Ltd, Beijing, China). In these experiments, all animal handlings were performed in accordance with European Commission guidelines (EEC Directive of 1986) to minimize the discomfort of the animals and were approved by the Animal Experimental Ethical Committee of Beijing University of Chinese Medicine. Isolation and culture of primary rat BMECs were performed as previous description [11, 13]. Briefly, the cerebral cortex of rats was isolated and grinded into small pieces. The brain gray matter was homogenized and filtered through meshes sequentially. The fragments were collected and digested with type II collagenase at 37 ° C for 20 min. Finally, the rat cerebral microvascular segments were collected and seeded in gelatin-coated dishes. Rat BMECs were also cultured in D-MEM/F-12 supplemented with 20% FBS, 0.86% endothelial cell growth supplement, 1% penicillin/streptomycin,0.5% insulin injection and 0.64% heparin sodium injection in a humidified incubator of 5% CO_2 at 37 °C. BMECs were grown to 80–90% confluency for passage. Finally, third generation rat BMECs (purity 98%) were used for the following experiments.

The necroptosis model of rat BMECs was established according to the method of our laboratory and other modeling techniques [11, 13–15]. In short, the BMECs were cultured with glucose-free Krebs solution containing 117.0 mM NaCl, 25 mM $NaHCO_3$,4.7 mM KCl, 2.5 mM $CaCl_2$,1.2 mM KH_2PO_4,1.2 mM $MgCl_2$ in a three gas hypoxic incubator chamber (1% O_2, 95% N_2 and 5% CO_2) at 37 °C for 2 h, then cultured with D-MEM/F-12 basal medium without FBS in 21.7% O_2 and 5% CO_2 normoxic

incubator at 37 °C for 8 h as resupply. Apoptosis inhibitor z-VAD-FMK (20μM) was added 30 min before and during the OGD/R induction. Z-VAD-FMK can block the apoptosis pathway and finally induce the occurrence of necroptosis [16].

Groups and Drug Administration

The BMECs were divided into 4 groups: (1) Control group: BMECs incubated in normal conditions. (2) OGD/R + z-VAD-FMK group: BMECs incubated according to the above method; (3) OGD/R + z-VAD-FMK + PNS group: BMECs were treated with 22 μg/ml PNS before and during the necroptosis model induction (which is the optimal concentration of PNS determined in our previous study) [11, 13]; (4) OGD/R + z-VAD-FMK + Nec-1(positive control) group: BMECs were treated with 10μM Nec-1 before and during the necroptosis model induction (which is the optimal concentration of Nec-1 determined in our previous study) [14]. The small molecule compound Nec-1 is a highly specific RIP1 kinase inhibitor and necroptosis inhibitor [17].

Cell Viability Analysis

Rat BMECs were inoculated into 96 well plates for OGD/R injury or drug treatment. 1/10 volume of CCK-8 solution was added to each well at 37 ºC and cultured in the dark for about 2 h. Finally, rat BMECs viability were measured at 450 nm by a microplate reader (Bio-Rad, Hercules, CA, USA).

Ultrastructural Analysis

Rat BMECs cultured in 25 cm^2 cell culture flasks were digested and centrifuged, then fixed in 2.5% cold glutaraldehyde with 1% osmium acid solution for 10 h at 4 ºC. The rat BMECs were sequentially dehydrated and embedded in epoxy resin. The block was cut to a thickness of 70–80 nm thickness using an ultrathin microtome. The slices were stained according to standardized preparation procedures. Ultrastructural analyses of the BMECs were performed using a transmission electron microscope (TEM) (H-7650, Hitachi, Tokyo, Japan).

Annexin V-FITC/PI Double Staining

After collecting of rat BMECs on 6 well culture plates, cells were washed twice with ice-cold D-Hank's and centrifuged at 200 g for 5 min. Then, the cells were suspended in Annexin V-FITC binding buffer and PI solution at room temperature for 15 min, according to the manufacturer's instructions. Necroptosis cells were detected using a flow cytometry (FACS Aria III, BD Biosciences, USA) and analyzed using FlowJo software.

Quantitative Real-time Polymerase Chain Reaction (qRT-PCR)

Total RNA was extracted from BMECs using TRIzol-Reagent (Invitrogen, Carlsbad, CA, USA) and subjected to reverse transcription. Thereafter, the first complementary DNA (cDNA) was synthesized using a Revert Aid First Strand cDNA Synthesis kit (Thermo Fisher Scientific Inc., USA). cDNA amplification was carried out using SYBR™ Green PCR Master Mix (Invitrogen, Carlsbad, CA, USA) on an ABI 7500 PCR instrument (Applied Biosystems, New York, USA). The cDNA was denatured by 39 PCR cycles (95 °C, 1 min; 94 °C, 30 s; 60 °C, 30 s; 72 °C, 15 s). The PCR primers were designed and synthesized by Invitrogen, and the sequences are listed in Table 1. β-actin was the invariant control, and the relative level of mRNA were calculated using the $2^{-\Delta\Delta Ct}$ method.

Western Blotting (WB)

BMECs were collected rapidly by scraping with ice-cold RIPA lysis buffer containing the protease inhibitor cocktail. Total protein concentrations were evaluated by using the bicinchoninic acid (BCA) protein assay kit. An equal amount of cell lysates was separated with 10% SDS-PAGE gel and then subsequently transferred to a polyvinylidene difluoride (PVDF) membrane (Merck Millipore, Billerica, MA, USA). These membranes were blocked with 5% nonfat dried milk or bovine serum albumin (BSA) for 2 h and incubated with the following primary antibodies: RIP1(1:1000), p-RIP1(Ser166) (1:1000), RIP3(1:1000), p-RIP3(T231 + S232) (1:1000), MLKL (1:1000), p-MLKL (Ser358) (1:1000), PGAM5 (1:500) and Drp1 (1:1000) at 4 °C overnight. β-actin was used

Table 1 The sequences of qRT-PCR primers

Gene	Forward	Reverse
RIP1	GAGGAGGAAAGGAAGCGAAG	TGACTGGTTGTGCTGGGATA
RIP3	GCTTGAACCCTTCGCTACTG	GACTGTGACCCTCCCTGAAA
MLKL	AGCCTCCCCAGTGACATTAC	GCCCACAGTAGCAAACTTCC
β-actin	TATCGGCAATGAGCGGTTCC	AGCACTGTGTTGGCATAGAGG

as a loading control. Next day, the PVDFs were washed and incubated with secondary antibodies (goat anti-rabbit IgG 1:5000 and goat anti-mouse IgG 1:5000) for 1.5 h at room temperature. The protein bands were visualized with high sensitivity chemiluminescence (ECL) detection kit (PIERCE, Massachusetts, USA) and exposure to the X-ray film.

Mitochondrial Membrane Potential (Δψm)

BMECs were seeded in a culture dish. Then, a single-cell suspension in PBS was prepared. After centrifugation and counting, BMECs were resuspended in culture medium and stained with Δψm assay kit with JC-1 (Beyotime, Shanghai, China) following the manufacturer's instruction. To examine the sensitivity of JC-1, 10μM of carbonyl cyanide 3-chlorophenylhydrazone (CCCP) were incubated with the rat BMECs that were treated without any drug before treatment of JC-1 at 37 °C for 20 min. The BMECs were analyzed using a flow cytometry (FACS Aria III, BD Biosciences, USA) to detect the red fluorescence exhibited by JC-1 aggregates (higher membrane potentials) and the green fluorescence exhibited by JC-1 monomers (lower membrane potentials). The Δψm was evaluated using the ratio of red/green fluorescence intensity.

BMECs were also seeded the density of at 1×10^5 cells/mL in a confocal dish. As described above, BMECs were washed with PBS and incubated with 5μM JC-1 probe. The depolarization ratio of Δψm was analyzed using a fluorescence microscopy (Olympus, Tokyo, Japan).

Statistical Analysis

All the measurement data were presented as mean ± standard deviation (SD) and were analyzed using SPSS 23.0 software (SPSS Inc., Chicago, IL, USA). The significant differences among the groups were evaluated using independent-tests, non-parametric test and one-way analysis of variance (ANOVA). P values < 0.05 were regarded as statistically significant. All experiments were performed independently in triplicate. Data from immunoreactivity quantification were analyzed and calculated using GraphPad Prism 8 (GraphPad Inc. San Diego, USA).

Results

PNS Improved Viability in OGD/R in Combination with z-VAD-FMK-Induced Rat BMECs

It has been reported that pan-caspase inhibitor z-VAD-FMK could induce necroptosis [18], so BMECs necroptosis was induced by OGD/R in combination with z-VAD-FMK. The shape of cell exposed to each treatment was shown in Fig. 1a. The cells were shrunk, rounded and fallen off after OGD/R in combination with z-VAD-FMK intervention, which was improved by PNS intervention. As shown in Fig. 1b, substantial cell death was detected in OGD/R + z-VAD-FMK group compared with the control group ($P < 0.01$). BMECs death was inhibited by RIP1 inhibitor Nec-1 ($P < 0.01$), suggesting that the cells died through the necroptosis pathway. Similar to Nec-1, PNS also significantly increased the viability of OGD/R in combination with z-VAD-FMK-induced BMECs (Fig. 1b).

PNS Reduced Necroptosis in OGD/R in Combination with z-VAD-FMK-Induced Rat BMECs

First, we performed Annexin V-FITC/PI double staining to detect the cell death modality induced by OGD/R in combination with z-VAD-FMK. As shown in Fig. 1c, the ratio of cells in the Q1, Q2, and Q4 quadrants of the OGD/R + z-VAD-FMK group was significantly increased compared with the control group ($P < 0.05$). Q1 quadrant normally represents the ratio of early apoptotic cells. Q2 quadrant is cells with positive annexin V-FITC and PI staining, which generally represent late apoptotic cells. After caspase was blocked, z-VAD-FMK induced necroptosis by phosphorylation RIP3, and the Annexin V-FITC and PI staining were also double positive in necroptosis cells. Therefore Q2 quadrant represents the late apoptosis and necroptosis of BMECs in this experiment. The cells ratio in Q2 quadrants was significantly decreased by Nec-1 intervention ($P < 0.05$), suggesting that necroptosis occurred in the OGD/R + z-VAD-FMK group. The ratio of Q2 quadrant cells was also significantly decreased in OGD/R + Z-VAD-FMK + PNS group ($P < 0.05$).

Then, the morphology of BMECs was observed by TEM (Fig. 1d). Intact nuclear membrane, clear cell nucleolus, abundant cytoplasm and organelles could be observed in the normal BMECs. While cells in OGD/R + z-VAD-FMK group displayed swelled organelles, ruptured cell membrane, decomposed cytoplasm and nucleus, which were consistent with the characteristics of necroptosis [19–22]. Interestingly, PNS or Nec-1 treatment reduced mitochondrial swelling, organelle damage and improved the integrity of nucleus and cell membrane in BMECs as shown in Fig. 1d. The flow cytometry and TEM results showed that PNS intervention significantly inhibited BMECs necroptosis induced by OGD/R in combination with z-VAD-FMK.

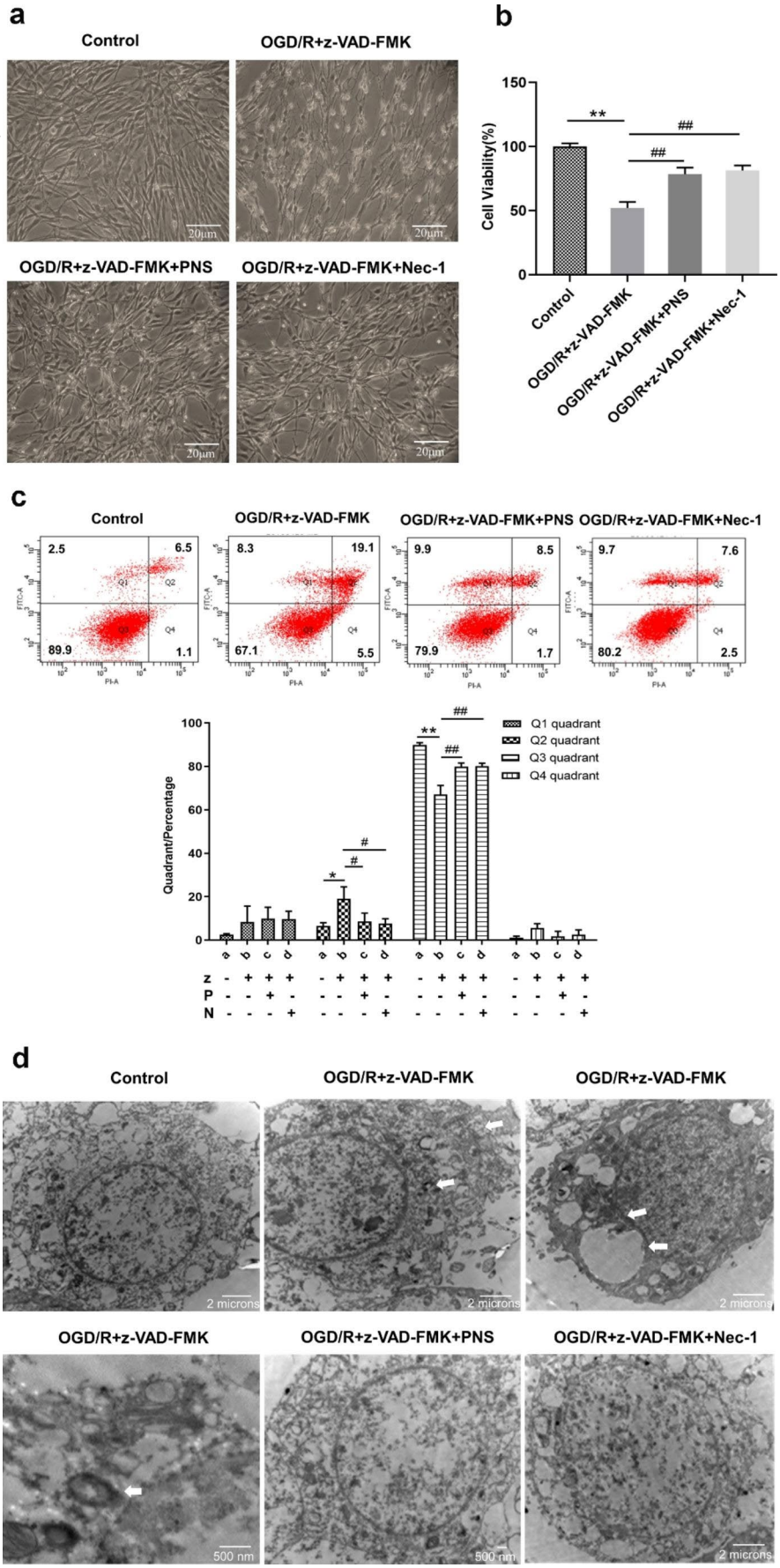

Fig. 1 The effect of PNS on the necroptosis in OGD/R in combination with z-VAD-FMK-induced rat BMECs. The injured BMECs were administrated with 22 μg/ml PNS. Nec-1was used as a positive control. (**a**) Phase contrast image of rat BMECs exposed to each treatment. (200× magnification, scale bar = 20 μm) (**b**) Bar graphs show the cell viability measured by CCK-8. (**c**) Annexin V-FITC/PI staining were used to detect the survival and death modality of BMECs induced by OGD/R in combination with z-VAD-FMK. z: z-VAD-FMK; P: PNS; N: Nec-1. Q1: early apoptotic cells; Q2: necroptosis cells and late apoptotic cells;Q3: normal (living) cells; Q4: necrotic cells. (**d**) Ultrastructural analyses of the BMECs were performed using TEM. The control BMECs showed normal cell nucleus and organelles (upper left panel, 10,000 × magnification, scale bar = 2 microns).Necroptosis cells showed swelled organelles, minor ultrastructural modifications of the nucleus and disrupted plasma membrane (upper panel, middle: 12,000× and right: 12,000 × magnifications, scale bar = 2 microns; lower left panel, 40,000× magnification, scale bar = 500 nm). Arrowheads point to damaged mitochondria, nucleus and cell membrane. The ultrastructure of BMECs in PNS (lower middle panel, 15,000× magnification, scale bar = 500 nm) or OGD/R + z-VAD-FMK + Nec-1 (lower right panel, 12,000× magnification, scale bar = 2 microns) group was improved. The data are presented as means ± S.D of three independent experiments. $^{*}P < 0.05$, $^{**}P < 0.01$ vs. control group, $^{\#}P < 0.05$, $^{\#\#}P < 0.01$ vs. OGD/R + z-VAD-FMK group

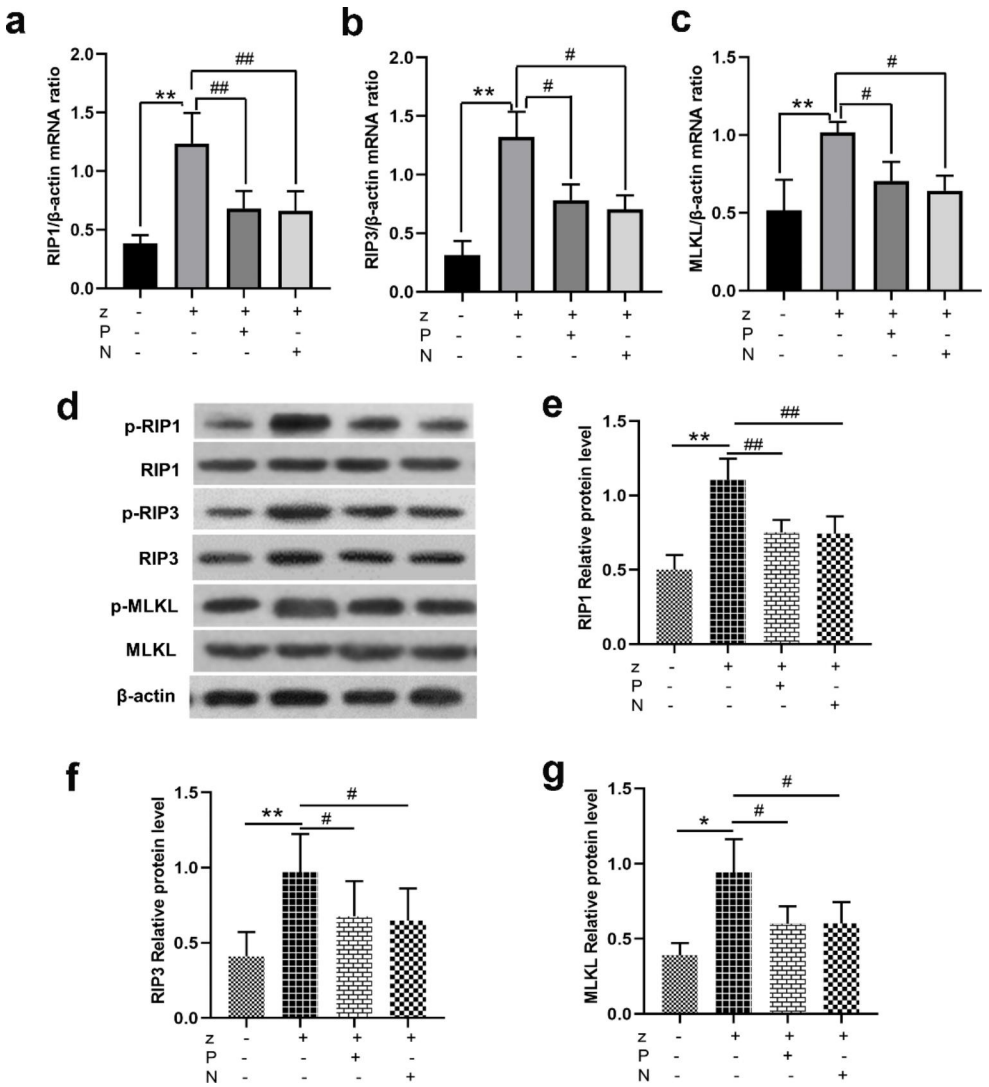

Fig. 2 The effect of PNS on RIP1-RIP3-MLKL signaling pathway in OGD/R in combination with z-VAD-FMK induced BMECs. The mRNA levels of RIP1(**a**), RIP3(**b**), MLKL(**c**) in BMECs were determined by qRT-PCR, respectively. (**d**)WB images of p-RIP1, RIP1, p-RIP3, RIP3, p-MLKL, MLKL and β-actin. (**e**, **f**, **g**) Bar graphs show ratios of phosphorylated protein/total protein. z: z-VAD-FMK; P: PNS; N: Nec-1. All the results were shown as mean ± S.D. The experiment was repeated three times. $^{*}P<0.05$, $^{**}P<0.01$ vs. control group, $^{\#}P<0.05$, $^{\#\#}P<0.01$ vs. OGD/R + z-VAD-FMK group

PNS Down-regulated the Phosphorylation of RIP1-RIP3-MLKL Signaling Pathway in BMECs

It was known that the RIP1-RIP3-MLKL signaling pathway has an important impact on the occurrence of necroptosis. We measured the mRNAs and proteins phosphorylation of RIP1, RIP3, MLKL by qRT-PCR and WB. Due to the limitation of experimental reagents, no phosphorylated antibody corresponding to the reaction source of rats was purchased. Human microvascular endothelial cell lines (HBMECs) were used in WB experiments to detect the phosphorylation levels of RIP1 at Ser166, RIP3 at T231 + S232, and MLKL at Ser358, respectively. We found that the mRNA levels of RIP1, RIP3, and MLKL were significantly increased in OGD/R in combination with z-VAD-FMK-induced BMECs (Fig. 2a, b and c) ($P<0.01$). Despite the similar expression levels of total RIP1, RIP3, and MLKL among the control and OGD/R + z-VAD-FMK groups, there was significant difference in the ratio of p-RIP1/RIP1, p-RIP3/RIP3 and p-MLKL/MLKL between the two groups (Fig. 2d, e and f, g) ($P<0.05$, $P<0.01$). These data suggested that RIP1-RIP3-MLKL signaling was activated by phosphorylation and mediated necroptosis in OGD/R in combination with z-VAD-FMK-induced BMECs. As shown in Fig. 2d, e and f, g, PNS treatment remarkably decreased the RIP1,

RIP3, and MLKL mRNA and proteins phosphorylation level ($P < 0.05$, $P < 0.01$). Similar results were observed in OGD/R + z-VAD-FMK + Nec-1 group.

PNS Inhibited the Expression of Downstream PGAM5 and Drp1 in BMECs

Recent studies have shown that the RIP1/RIP3 necrosome has been proposed to activate phosphoglycerate mutase 5 (PGAM5), an atypical mitochondrial Ser/Thr phosphatase. PGAM5 recruits and activates the mitochondrial fission factor dynamin-related protein 1 (DrP1) to cause mitochondrial fragmentation and RIPK1-RIPK3-MLKL subsequently mediated necroptosis [23, 24].To investigate whether PGAM5 and Drp1 involved in OGD/R in combination with z-VAD-FMK-induced BMECs necroptosis, we measured the expression levels of PGAM5 and Drp1 mRNAs and proteins by qRT-PCR and WB. The results showed that mRNA and protein expression of PGAM5 (Fig. 3a and c) and Drp1 (Fig. 3b and d) in OGD/R in combination with z-VAD-FMK-induced BMECs were significantly raised compared with the normal BMECs, whereas Nec-1 markedly declined the level of PGAM5 and Drp1 ($P < 0.05$, $P < 0.01$), which indicate that activation of RIP1-RIP3-MLKL induced expression of PGAM5 and Drp1 in model BMECs. In contrast, these parameters came to a lower level in OGD/R + Z-VAD-FMK + PNS group than OGD/R + z-VAD-FMK group, showing PNS inhibited the activation of PGAM5 and Drp1 in OGD/R in combination with z-VAD-FMK-induced BMECs.

PNS Reduced the Damage of Δψm in Rat BMECs

Indeed, non-canonical signaling pathways, such as the RIP1-RIP3-MLKL-PGAM5-Drp1 mediated mitochondrial fission [25, 26] have been reported. The Δψm is an important parameter of mitochondrial function, which is also used as an indicator of cell viability and changes when necroptosis occurs. Next, the Δψm was assessed by JC-1 dye. In a JC-1 assay, dyes would gather in the mitochondria and emit red fluorescence in normal cells. When the Δψm is depolarized, JC-1 is released from the mitochondrial matrix, and exists in the cytoplasm in the form of monomer and emits green fluorescence. The results showed the percentage of cells in the P2 region emitting red fluorescence was high in normal group. The number of cells in the P2 region decreased in OGD/R + z-VAD-FMK group ($P < 0.01$), with weak red fluorescence (Fig. 3f-b1) and strong green fluorescence (Fig. 3f-b2) by fluorescence microscopy, suggesting Δψm decreased after modeling. PNS or Nec-1 treatment reversed the mitochondrial depolarization ($P < 0.05$) (Fig. 3e, f-c and f-d). These data sets indicated that PNS protected the mitochondrial function in OGD/R in combination with z-VAD-FMK-induced BMECs.

Discussion

In 2005, Degterev et al. [3] found that the absence of caspase signal transduction factors in cells, a series of molecular control signal, can produce a new way of cell death. The novel manner of cell death has the morphological characteristics of necrotic cells and similar mechanism to apoptotic cells, officially named as necroptosis. This started the study in programmed necrosis. According to recent studies, necroptosis has the following characteristics[27–32]: (1) It exhibits obvious morphological changes of cell necrosis, including organelle swelling, destruction of cell membrane integrity, loss of cell content logistics and infiltration and activation of inflammatory cells, etc. (2) Necroptosis is a form of programmed cell death not mediated by caspases, instead, initiated by the receptor and non-receptor molecules and the signaling molecules involved RIP1, RIP3, PARP-1, Ca^{2+}, etc. (3) It can be induced by the caspase blocker z-VAD-FMK. Z-VAD-FMK is a synthetic broad-spectrum caspase inhibitor, which can block the occurrence of apoptosis pathway and finally induce the occurrence of necroptosis. (4) It can be specifically inhibited by the small molecule compound Nec-1, a specific inhibitor of RIPK1, which has no effect on apoptosis.

Increasing evidence showed that necroptosis contributes to delaying brain injury in cerebral ischemia and could be a new therapeutic target for stroke[33]. In this study, the necroptosis model of BMECs was induced by OGD/R in combination with z-VAD-FMK based on previous experiments. At present, there is no specific marker to directly mark necroptosis. Therefore, three experiments were conducted to evaluate the pharmacological effects of PNS on necroptosis. First BMECs viability was examined by CCK-8. The results showed the viability of cells in the OGD/R + z-VAD-FMK group (51.4%) decreased significantly, while PNS (78.4%) reversed this effect and improved the viability in OGD/R in combination with z-VAD-FMK induced BMECs. CCK-8 assay only represents the cells viability, but it can't explain the specific form of cell death. Annexin V-FITC/PI double staining method was used to detect the form of cell death by flow cytometry. Annexin V-FITC can bind to the phosphatidylserine which has been transferred to the cell surface in the early stage of apoptosis. Therefore, the positive expression of Annexin

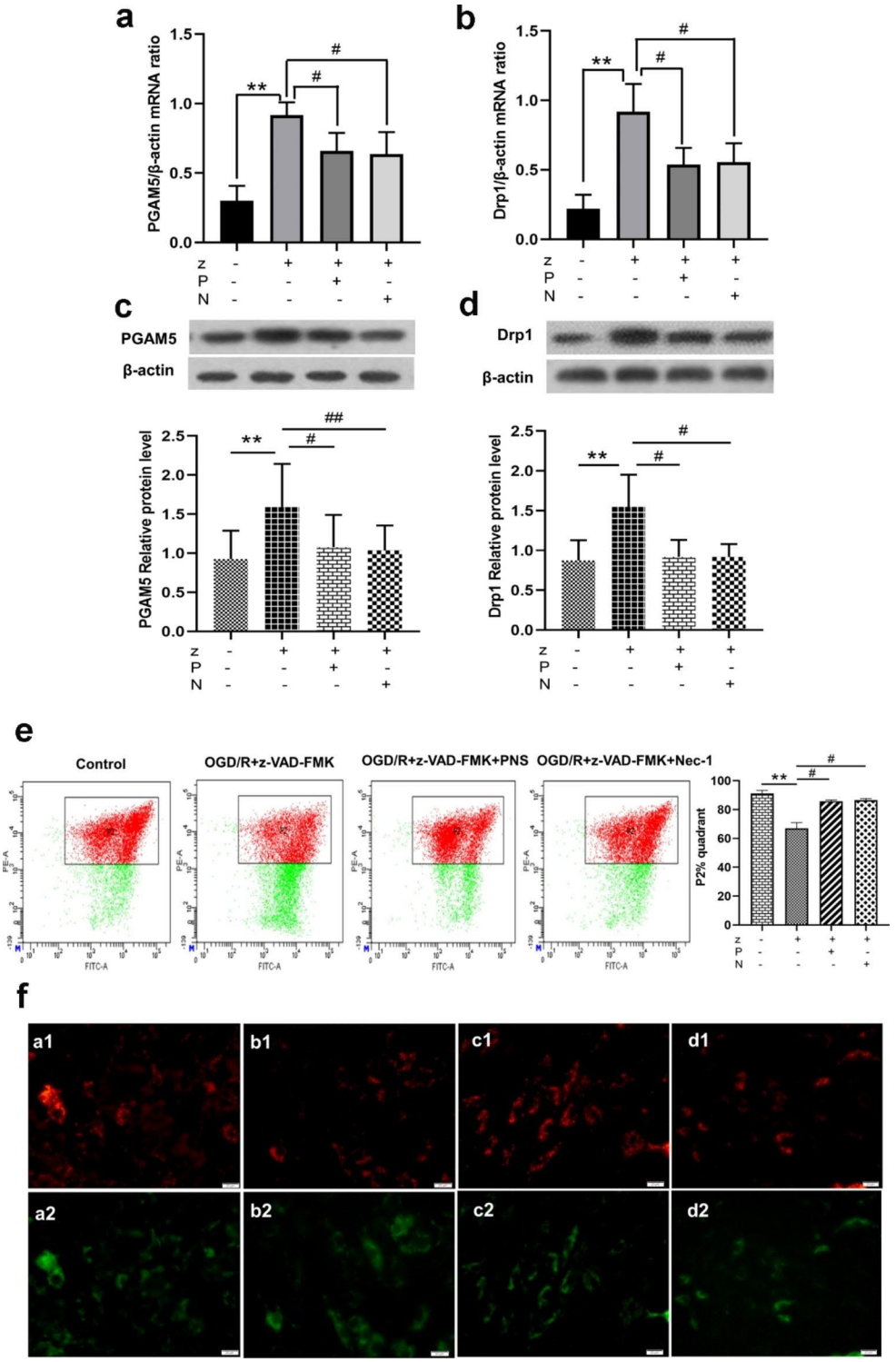

Fig. 3 The effect of PNS on the expression of PGAM5, Drp1 and Δψm in OGD/R in combination with z-VAD-FMK induced BMECs. PGAM5(**a**, **c**), Drp1(**b**, **d**) mRNA and protein expression were determined by qRT-PCR and WB. z: z-VAD-FMK; P: PNS; N: Nec-1. (**e**) Δψm of BMECs were analyzed using flow cytometry. The percentage of cells in the P2 region emitting red fluorescence was evaluated. (**f**) The depolarization of Δψm was observed by fluorescence microscopy (200× magnification, scale bar = 20 μm). Red fluorescence suggested normal Δψm, and green fluorescence indicated Δψm decrease or loss. (a1,a2): control group; (b1,b2): OGD/R + z-VAD-FMK group; (c1,c2): OGD/R + z-VAD-FMK + PNS group; (d1,d2): OGD/R + z-VAD-FMK + Nec-1 group. Data are presented as mean ± S.D. All experiments were repeated three times. $^{*}P < 0.05$, $^{**}P < 0.01$ vs. control group, $^{\#}P < 0.05$, $^{\#\#}P < 0.01$ vs. OGD/R + z-VAD-FMK group

V-FITC can be used as one of the sensitive indicators for detecting early cell apoptosis. Z-VAD-FMK mainly inhibits apoptosis by blocking caspase and has little effect on early apoptosis. In this experiment, the cells ratio in Q1 quadrants increased in OGD/R + z-VAD-FMK group. PNS slightly reduced the proportion of Q1 cells, but there was no significant difference between the OGD/R + Z-VAD-FMK + PNS groups and the OGD/R + z-VAD-FMK group. Q2 quadrant showed cells with positive annexin V-FITC and PI staining and represented the late apoptosis or necroptosis of BMECs. The cells ratio in Q2 quadrants was significantly decreased by Nec-1 intervention, suggesting that necroptosis occurred in the OGD/R + z-VAD-FMK group. PNS significantly decreased the ratio of Q2 quadrant cells, indicating PNS reduced the necroptosis in OGD/R in combination with z-VAD-FMK induced BMECs. In order to confirm that necroptosis was the cell death form of PNS intervention, we observed the ultrastructural changes of cells in each group by TEM. The results showed that the plasma membrane was dissolved, the contents released from the cell, the mitochondria swollen, and the nuclear membrane was basically intact in the OGD/R + z-VAD-FMK group. These morphological changes indicated characteristics of necroptosis. After the intervention of PNS and Nec-1, the structural damage of rat BMECs in the two groups was improved. The results of the above three experiments suggested PNS has a significant inhibitory effect on rat BMECs necroptosis induced by OGD/R in combination with z-VAD-FMK.

Many extracellular and intracellular stimuli has been found as the activation of necroptosis signaling pathways. Among them, necroptosis induced by death receptor activation is the most extensive and hot topic research. Upon the death receptors activated, many downstream molecules are recruited in an organized order. It is known that TNF triggers the formation of a TNF receptor 1 (TNFR1) signaling complex (Complex I) by recruiting several effectors such as TNFR-associated factor 2 (TRAF2), cellular inhibitor of apoptosis proteins 1 (cIAPs) and RIP1. RIP1 is an upstream regulator of the necroptosis pathway. In certain pathological conditions, the de-ubiquitination of RIP1, TRADD, RIP3 and caspase-8 form complex II, which could lead to caspase activation and subsequent apoptosis. In the setting of caspase-8 deficiency or inactivation, RIP1 are phosphorylated at Ser14, Ser15, Ser20, Ser161 or Ser166 sites and RIP3 are phosphorylated at Thr231 and Ser232 sites [34, 35], leading to the activation of MLKL via phosphorylation at Thr357 and Ser358 [36]. Then p-MLKL undergoes oligo-merization and causes cell necroptosis via binding to phosphatidylinositol phosphates in the plasma membrane, causing membrane permeabilization. In addition, activated MLKL is also recruited to the mitochondrial membrane, leading to mitochondrial dysfunction [37]. Therefore, phosphorylation of RIP1-RIP3-MLKL signaling pathway is generally considered to be a marker of cell necroptosis. In the present study, the mRNA and phosphorylated protein levels of RIP1, RIP3 and MLKL were measured by qRT-PCR and WB, respectively. Our results showed phosphorylation of RIP1-RIP3-MLKL pathways increased in OGD/R + z-VAD-FMK group, which could be blocked by Nec-1, suggesting the RIP1-RIP3-MLKL signaling pathway participates in the occurrence of necroptosis in OGD/R in combination with z-VAD-FMK-induced injury. PNS markedly reduced phosphorylation of RIP1-RIP3-MLKL, showing the similar effect with Nec-1, which suggested that PNS may inhibit the occurrence of necroptosis by modulating RIP1-RIP3-MLKL signaling pathway.

It was reported that PGAM5, a 32 kDa mitochondrial membrane protein with homology to a family of phosphoglycerate mutases that associates with RIP1-RIP3-MLKL complex, promotes necroptosis [38]. Furthermore, PGAM5 has been implicated in mitochondria fission through dephosphorylation and activation of the mitochondrial fission protein DrP1 [39]. It was also reported that Drp1-mediated mitochondrial fragmentation is essential to necroptosis [40]. These molecules could destroy mitochondria and ultimately cause cell death. In the present study, cells were stained with JC-1 to detect the changes of $\Delta\psi m$, which was the most important manifestation of mitochondrial dysfunction. The results showed that the mRNA and protein levels of PGAM5 and Drp1 were significantly up-regulated, while the $\Delta\psi m$ decreased in OGD/R in combination with z-VAD-FMK-induced BMECs. PNS or Nec-1 treatment significantly suppressed the expression of PGAM5 and Drp1 and improved $\Delta\psi m$. The data elucidated the protective effect of PNS on necroptosis of rat BMECs induced by OGD/R in combination with z-VAD-FMK.

In conclusion, the necroptosis of BMECs could be induced by OGD/R in combination with z-VAD-FMK. PNS can effectively reduce the occurrence of BMECs necroptosis, and its intrinsic mechanism is related to the inhibition of RIP1-RIP3-MLKL signaling pathway, decreasing the expression of PGAM5 and Drp1, and mitigating mitochondrial damage (Fig. 4). Therefore, our study provides the evidence supporting PNS as a potential drug for anti-necroptosis and endothelial protection in ischemic diseases. But the findings around an artificial in vitro model of necroptosis was bit limited. We will test our hypothesis in an experimental ischemia/reperfusion model in vivo i.e., MCAO and explore how PNS treatment may salvage from necroptosis cell death and the molecular mechanisms involved in the future.

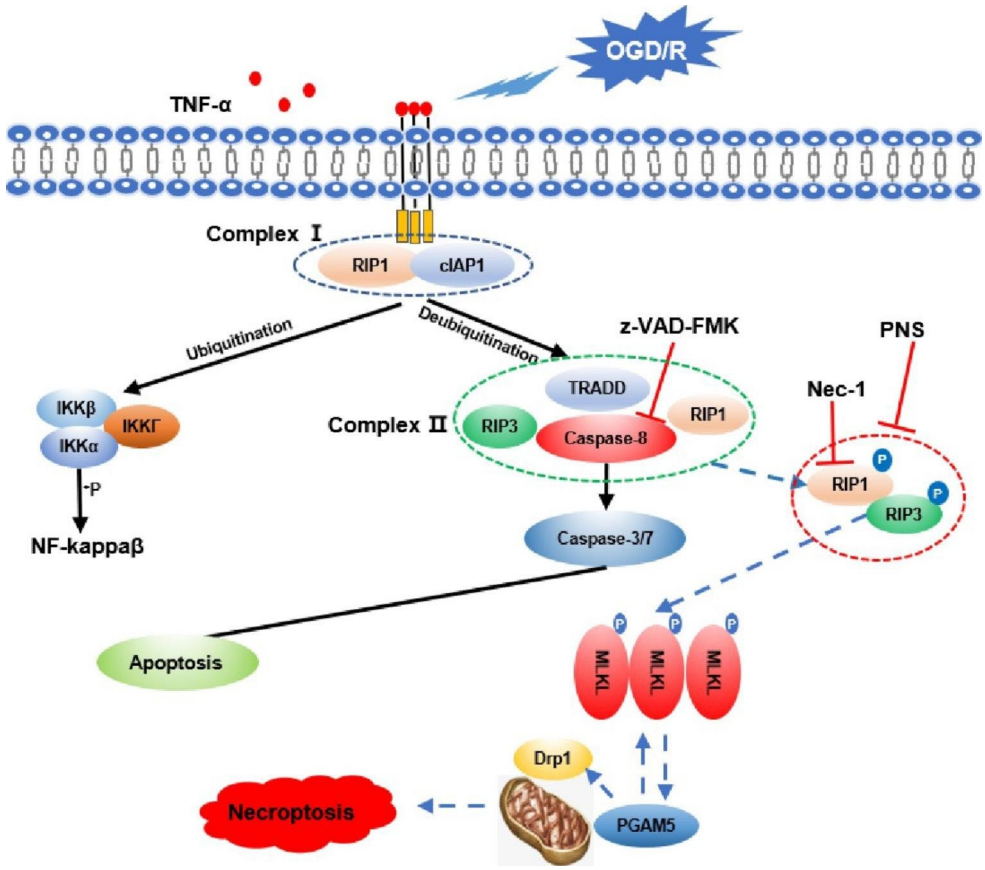

Fig. 4 A proposed schematic diagram of the PNS protection on BMECs necroptosis. OGD/R in combination with z-VAD-FMK induced BMECs necroptosis signaling transduction, including necrosome formation and phosphorylation of RIP1, RIP3 and MLKL. The activation of PGAM5 facilitated mitochondria damage, promoting necroptosis and aggravating OGD/R by activation of DrP1. PNS inhibited the RIP1-RIP3-MLKL signaling pathway, decreased the expression of PGAM5 and Drp1, and maintained mitochondrial homeostasis

Supplementary Information The online version contains supplementary material available at https://doi.org/10.1007/s11064-022-03675-0.

Acknowledgements The authors would like to acknowledge financial support from the National Natural Science Foundation of China (Grant No.82104673,81273885) and The Fundamental Research Funds for the Central Public Welfare Research Institutes (Grant No. ZZ15-YQ-056).

Author Contributions YH performed all experiments and wrote the manuscript; SZ, JM, SK, LW, FL, FZ, TS and CZ helped with the biological study and data statistics; WL conducted and supervised the whole experiments. All authors read and approved the final manuscript.

Data Availability The datasets generated during and/or analysed during the current study are available from the corresponding author on reasonable request.

Declarations

Conflict of interest The authors declare that they have no conflicts of interest.

References

1. Benjamin EJ, Muntner P, Alonso A et al (2019) Heart disease and stroke statistics—2019 update: a report from the American Heart Association. Circulation 139:e56–e528
2. Chen AQ, Fang Z, Chen XL et al (2019) Microglia-derived TNF-α mediates endothelial necroptosis aggravating blood brain–barrier disruption after ischemic stroke. Cell Death Dis 10:487
3. Degterev A, Huang Z, Boyce M et al (2005) Chemical inhibitor of nonapoptotic cell death with therapeutic potential for ischemic brain injury. Nat Chem Biol 1:112–119
4. Naito MG, Xu D, Amin P et al (2020) Sequential activation of necroptosis and apoptosis cooperates to mediate vascular and neural pathology in stroke. Proceedings of the National Academy of Sciences 117: 4959–4970
5. Wehn AC, Khalin I, Duering M et al (2021) RIPK1 or RIPK3 deletion prevents progressive neuronal cell death and improves memory function after traumatic brain injury. Acta Neuropathol Commun 9:1–18
6. Zhang Y, Li K, Wang X et al (2021) CSE-Derived H2S Inhibits Reactive Astrocytes Proliferation and Promotes Neural Functional Recovery after Cerebral Ischemia/Reperfusion Injury in Mice Via Inhibition of RhoA/ROCK2 Pathway. ACS Chem Neurosci 12:2580–2590

7. Sun T, Wang P, Deng T et al (2021) Effect of Panax notoginseng Saponins on Focal Cerebral Ischemia-Reperfusion in Rat Models: A Meta-Analysis. Front Pharmacol 11:2491
8. Zhang J, Guo F, Zhou R et al (2021) Proteomics and transcriptome reveal the key transcription factors mediating the protection of Panax notoginseng saponins (PNS) against cerebral ischemia/reperfusion injury. Phytomedicine 92:153613
9. Geng H, Zhang L, Xin C et al (2021) Xuesaitong oral preparation as adjuvant therapy for treating acute cerebral infarction: A systematic review and meta-analysis of randomized controlled trials. J Ethnopharmacol 285:114849
10. Wang L, Xu Z, Liang X et al (2021) Systematic Review and Meta-Analysis on Randomized Controlled Trials on Efficacy and Safety of Panax Notoginseng Saponins in Treatment of Acute Ischemic Stroke. Evidence-Based Complementary and Alternative Medicine:4694076
11. Li W, Li P, Liu Z et al (2014) A Chinese medicine preparation induces neuroprotection by regulating paracrine signaling of brain microvascular endothelial cells. J Ethnopharmacol 151:686–693
12. Zhang C, Zhang S, Wang L et al (2021) The RIG-I Signal Pathway Mediated Panax notoginseng Saponin Anti-Inflammatory Effect in Ischemia Stroke. Evidence-Based Complementary and Alternative Medicine:8878428
13. Li W, Li P, Hua Q et al (2009) The impact of paracrine signaling in brain microvascular endothelial cells on the survival of neurons. Brain Res 1287:28–38
14. Hu Y, Lei H, Wang S et al (2017) The Establishment of Necroptosis Model on Mimic Ischemic Reperfusion Injury in Brain Microvascular Endothelial Cells. World Chin Med 12:879–883
15. Uzunparmak B, Gao M, Lindemann A et al (2020) Caspase-8 loss radiosensitizes head and neck squamous cell carcinoma to SMAC mimetic–induced necroptosis. JCI insight 5:e139837
16. Yuan Z, Yi YS, Hai YY (2020) Triad3A displays a critical role in suppression of cerebral ischemic/reperfusion (I/R) injury by regulating necroptosis. Biomed Pharmacother 128:110045
17. Zhu YM, Lin L, Wei C et al (2021) The Key Regulator of Necroptosis, RIP1 Kinase, Contributes to the Formation of Astrogliosis and Glial Scar in Ischemic Stroke. Translational Stroke Research 12:991–1017
18. Zhou T, DeRoo E, Yang H et al (2021) MLKL and CaMKII Are Involved in RIPK3-Mediated Smooth Muscle Cell Necroptosis. Cells 10:2397
19. de Almagro MC, Vucic D (2015) Necroptosis: Pathway diversity and characteristics[C]//Seminars in cell & developmental biology. Acad Press 39:56–62
20. Verduijn J, Van der Meeren L, Krysko DV et al (2021) Deep learning with digital holographic microscopy discriminates apoptosis and necroptosis. Cell death discovery 7:1–10
21. Vandenabeele P, Galluzzi L, Vanden Berghe T et al (2010) Molecular mechanisms of necroptosis: an ordered cellular explosion. Nat Rev Mol Cell Biol 11:700–714
22. Linkermann A, Green DR (2014) Necroptosis. N Engl J Med 370:455–465
23. Zhu H, Tan Y, Du W et al (2021) Phosphoglycerate mutase 5 exacerbates cardiac ischemia-reperfusion injury through disrupting mitochondrial quality control. Redox Biol 38:101777
24. Xu Q, Guo J, Li X et al (2021) Necroptosis Underlies Hepatic Damage in a Piglet Model of Lipopolysaccharide-Induced Sepsis. Front Immunol 12:745
25. Cheng M, Lin N, Dong D et al (2021) PGAM5: a crucial role in mitochondrial dynamics and programmed cell death. Eur J Cell Biol 100:151144
26. Xue C, Gu X, Li G et al (2021) Mitochondrial mechanisms of necroptosis in liver diseases. Int J Mol Sci 22:66
27. Moujalled D, Strasser A, Liddell JR (2021) Molecular mechanisms of cell death in neurological diseases. Cell Death & Differentiation 28:2029–2044
28. Adameova A, Horvath C, Abdul-Ghani S et al (2022) Interplay of Oxidative Stress and Necrosis-like Cell Death in Cardiac Ischemia/Reperfusion Injury: A Focus on Necroptosis. Biomedicines 10:127
29. Hua X, Li B, Yu F et al (2022) Protective Effect of MFG-E8 on Necroptosis-Induced Intestinal Inflammation and Enteroendocrine Cell Function in Diabetes. Nutrients 14:604
30. Dong K, Zhu Y, Deng Q et al (2022) Salmonella pSLT-encoded effector SpvB promotes RIPK3-dependent necroptosis in intestinal epithelial cells. Cell Death Discovery 8:1–11
31. Kamiya M, Mizoguchi F, Kawahata K et al (2022) Targeting necroptosis in muscle fibers ameliorates inflammatory myopathies. Nat Commun 13:1–12
32. Das N, Samantaray S, Ghosh C et al (2022) Chimaphila umbellata extract exerts anti-proliferative effect on human breast cancer cells via RIP1K/RIP3K-mediated necroptosis. Phytomedicine Plus 2:100159
33. Tuo Q, Zhang S, Lei P (2022) Mechanisms of neuronal cell death in ischemic stroke and their therapeutic implications. Med Res Rev 42:259–305
34. Khuanjing T, Ongnok B, Maneechote C et al (2021) Acetylcholinesterase inhibitor ameliorates doxorubicin-induced cardiotoxicity through reducing RIP1-mediated necroptosis. Pharmacol Res 173:105882
35. Wu L, Chung JY, Cao T et al (2021) Genetic inhibition of RIPK3 ameliorates functional outcome in controlled cortical impact independent of necroptosis. Cell Death Dis 12:1–16
36. Seo J, Nam YW, Kim S et al (2021) Necroptosis molecular mechanisms: Recent findings regarding novel necroptosis regulators. Exp Mol Med 53:1007–1017
37. Huang HR, Cho SJ, Harris RM et al (2021) RIPK3 activates MLKL-mediated necroptosis and inflammasome signaling during Streptococcus infection. Am J Respir Cell Mol Biol 64:579–591
38. Liu Y, Xu Q, Wang Y et al (2021) Necroptosis is active and contributes to intestinal injury in a piglet model with lipopolysaccharide challenge. Cell Death Dis 12:1–14
39. Hu Y, Feng X, Chen J et al (2022) Hydrogenrich saline alleviates early brain injury through inhibition of necroptosis and neuroinflammation via the ROS/HO1 signaling pathway after traumatic brain injury. Experimental and therapeutic medicine 23:1–10
40. Lee AJ, Liao HJ, Hong JR (2022) Overexpression of Bcl2 and Bcl2L1 Can Suppress Betanodavirus-Induced Type III Cell Death and Autophagy Induction in GF-1 Cells. Symmetry 14:360